Inelastic π^+ scattering from ^{12}C and Si at low energies

J. F. Amann,* P. D. Barnes, K. G. R. Doss, S. A. Dytman,† R. A. Eisenstein, J. D. Sherman,* and W. R. Wharton

Physics Department, Carnegie-Mellon University, Pittsburgh, Pennsylvania 15213

(Received 30 October 1980)

Angular distributions for elastic and inelastic scattering of π^+ projectiles from natural carbon and silicon targets at energies of $\sim$35 and 68 MeV are reported. The elastic data, along with other reported low energy pion scattering data for ^{12}C, is fitted using the zero-range four-parameter (b_0, b_1) Kisslinger optical potential. The best-fit potential is found to be nearly independent of energy between 30 and 68 MeV, the largest energy dependence being in Re(b_0) which changes by 30%. Simple distorted-wave impulse approximation calculations which succeed in describing the 2^+ 4.4 MeV cross section at 48.5 MeV do much worse at 67.5 MeV for angles where the 2^+ cross section is comparable to or larger than the elastic cross section. This suggests that a coupled channels calculation is needed. The poor agreement between data and theory for the 0^+ (7.6 MeV) and 3^- (9.6 MeV) ^{12}C transitions found earlier at 48.5 MeV persists at 67.5 MeV. The shape of the pion energy spectra and the energy integrated inelastic angular distribution at 67.5 MeV is poorly described by a quasifree pion-nucleon scattering process.

> NUCLEAR REACTIONS Elastic and inelastic scattering of 35 and 68 MeV π^+
> from ^{12}C and ^{28}Si. Angular distributions: $25° \le \theta \le 150°$. Optical model and
> DWIA analysis of cross-section data.

I. INTRODUCTION

Low energy pion scattering studies have generated much interest in recent years.[1-4] Data for elastic scattering (mainly with π^+) have been published for a number of nuclei in the energy range 30–50 MeV.[5-7] All data for light nuclei show a characteristic minimum at 60°–65° that is apparently due to the zero in the pion-nucleon t matrix[8] rather than diffractive scattering from the nuclear surface. This minimum is deeper for π^- scattering than for π^+ and for both π^+ and π^- it becomes less prominent as the target mass increases. These features of the scattering can be described phenomenologically by a simple four-parameter Kisslinger potential, of either zero[5] or finite[7] range. Interestingly, the parameters for $N \sim Z$ nuclei are found to vary little from nucleus to nucleus.

Detailed optical model calculations[9-14] have shown rather strong sensitivity to various nuclear medium effects, including Fermi motion, binding, and correlations between nucleons. In addition, true π absorption is thought to be quite important. Thus, while there is disagreement in the specific nature of the individual calculations, it is clear that one must go well beyond the impulse approximation to fit the data. The elastic data are then excellent tests of the ability of any detailed microscopic theory using the multiple scattering series to predict low energy pion scattering cross sections. They also can provide useful distorted wave input for calculations involving pion reactions.

The ambiguities present in recent optical model calculations of elastic scattering reflect two concerns. First, different nuclear medium effects can produce similar (i.e., indistinguishable) changes in the calculated angular distribution, especially those involving second-order corrections. Often there is insufficient information available to treat such effects adequately. Second, there is the fundamental fact that elastic scattering measures only asymptotic phase shift information. Thus, a wide variety of phase shift equivalent potentials, which produce quite different pion wave functions inside the nucleus, will give the same elastic cross sections.[15] Both considerations suggest a wider program of interest.

The major subject of this work is the inelastic scattering of pions leaving the nucleus in either a bound or a continuum nuclear state. These data comprise a major portion of the reaction cross section and can test the pion wave function in the nuclear interior or surface region rather than asymptotically.

Inelastic scattering data at low energies are much more limited than for the elastic case; at present the only case[5] for which there exists a full angular distribution is the 2^+ state at 4.44 MeV in ^{12}C for 48.5 MeV π^+. As with elastic scattering, there is a minimum at $\sim$65°. A distorted-wave impulse approximation (DWIA) calculation reproduces these data only if a distorting potential is used that fits the elastic data well.

In this work, we explore the energy dependence of elastic and inelastic π^+ scattering from carbon

and silicon. Previously, we have published data
at ~50 MeV for each of these nuclei[5]; data at
~35 MeV (^{12}C, Si) and 67.5 MeV (^{12}C) will be re-
ported here. The data at 67.5 MeV represent a
step upward in energy from the low energy region
toward the resonance region where a quite dif-
ferent reaction mechanism dominates. Since a
long-term goal of pion physics is to construct a
unified theoretical description of data from
0–300 MeV, data in the "transition region" be-
tween low and resonance energy will hopefully
provide guidance in this matter. Another aspect
of our data is that the inelastic spectra obtained
at 67.5 MeV were measured up to 34 MeV excita-
tion energy in the residual system. Thus, energy-
integrated inelastic cross sections are also
available.

II. EXPERIMENTAL METHOD

The experimental setup for this work is similar
to that of Ref. 5. Figure 1 shows the apparatus
schematically. In the present experiment, the
pion beam used was the LEP channel at LAMPF.
With a 150 μA proton current, the channel pro-
vided ~2×10^6 π^+ per second at 69 MeV for a
typical momentum bite of $\frac{3\%}{4}$ and ~10^6 π^+/sec
at 37 MeV for a $\Delta p/p$ of 1%.

The targets used were of natural isotopic abun-
dance and of high chemical purity. The silicon
target was 180 mg/cm^2 in thickness, manufactured
from single-crystal detector material cut into
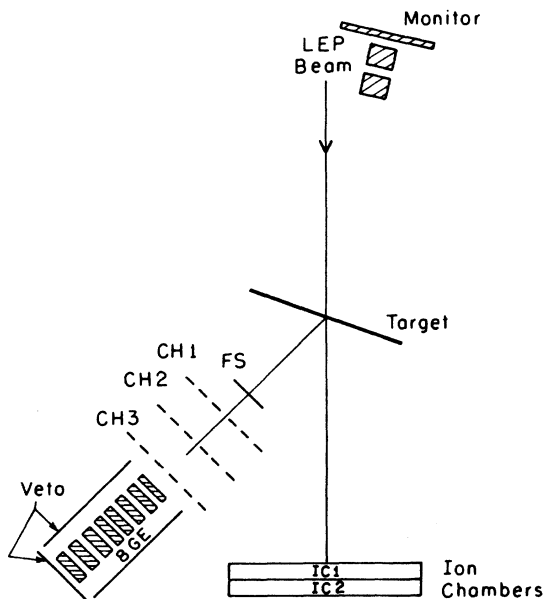4 cm squares and glued together. The glue repre-

FIG. 1. A schematic diagram of the apparatus used
in the experiment. The monitor telescope is in the ver-
tical plane 60° from the horizontal.

sented about 1% of the target mass and was there-
fore ignored in the analysis. The carbon targets
were made of graphite and varied in thickness
from 200 to 1000 mg/cm^2.

The detector arrangement (see Fig. 1) consisted
of a trigger scintillator, position chambers, and
a stopping detector. The central detection device
was a stack of eight highly pure germanium crys-
tals in a single cryostat. (This device was built
by the Lawrence Berkeley Laboratory Detector
Group and will be discussed in detail in a forth-
coming publication.) The first two crystals are
thinner (2.5 and 7.5 mm) than the other six
(1.2 cm each). Each crystal is 4 cm in diameter
and has a very thin (0.1 μm) Pd p contact on one
face with Li (50–100 μm) on the other face. An-
nular boron nitride rings, with a 3.5 cm diameter
hole, hold the crystals in place.

The energy deposited in each crystal by the in-
coming particle is measured and added to give
the total particle energy. The detector will stop
pions with kinetic energies less than 105 MeV
and protons with less than 220 MeV. Any particle
with a range larger than the thickness of the first
crystal (~2.5 mm Ge) or less than the thickness
of the full stack (~8 cm Ge) can be identified.
For pions, this corresponds to ~15–105 MeV.
However, background problems limited the data
for these inclusive measurements to pion energies
above ~28 MeV. (Since the time of this experi-
ment, however, we have developed techniques
to take data across the fully energy range for
pions. These will be described in a forthcoming
publication.[16])

The detector has excellent intrinsic resolution
but has a fairly complicated response function.
In most cases, a pion entering the detector will
deposit essentially all of its kinetic energy in the
active volume of the system. However, there are
a number of ways that a different amount of
charge can be collected. For example, the parti-
cle may multiple scatter out of the detector or
lose energy before stopping that is not collected
(e.g., photon emission). These problems have
been or will be discussed in detail in other pub-
lications.[5,17,18] Software cuts and corrections
must be utilized to identify and reject such
events; these result in some detector inefficiency.
The detector response function for monoenergetic
pions (elastic events from a lead target at a
forward angle) is shown in Fig. 2 of the last paper
in Ref. 5.

The biggest background in the event trigger
of a low energy pion scattering experiment is due
to nontarget-related events arising from pion or
muon decay in the beam near the target, with the
resultant muon or electron triggering the detec-

tion system. Such events can give a signal in the germanium detector similar to that of a pion and produce deadtime in the computer due to unwanted events. In the previous experiment,[5] wire chambers were used to plot each event's trajectory to the target region and determine if it came from the target. In this experiment, helical delay line wire chambers were used for this purpose again, and in addition, a 1.6 mm thick scintillator (FS) placed in front of the first wire chamber (CH1). To be analyzed in the computer, an event was required to fire FS in addition to the first two (three) germanium crystals for the data at 37 (69) MeV. This effectively localized the event to a space 10 cm wide around the target, cutting out almost all decay events from the trigger at the cost of worsening the total energy resolution by about 200 keV. The wire chambers were used to determine where the particle entered the front face of the first crystal. By requiring the radius of entry to be less than 1.5 cm, events that pass through the boron nitride mounting ring are discriminated against. This cut is essential to make the peak shape clean enough to extract inelastic cross sections with 1% as many counts as the elastic. Figures 2, 3, and 4 show examples of spectra at each energy. The data at 67.5 MeV includes inelastic pions leaving the nucleus at up to ~34 MeV excitation energy. These spectra have been corrected for varying detector efficiency with energy using a method described below.

Inelastic peak areas were extracted in the same way as for the 48.5 MeV data.[5] Background from the elastic peak was estimated by eye, consistent with the measured monoenergetic peak shape. The inelastic to elastic cross section ratio was then determined by counting events within an
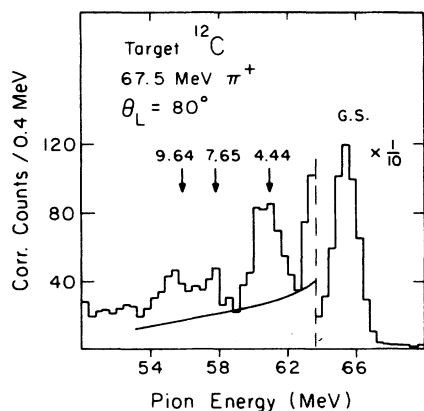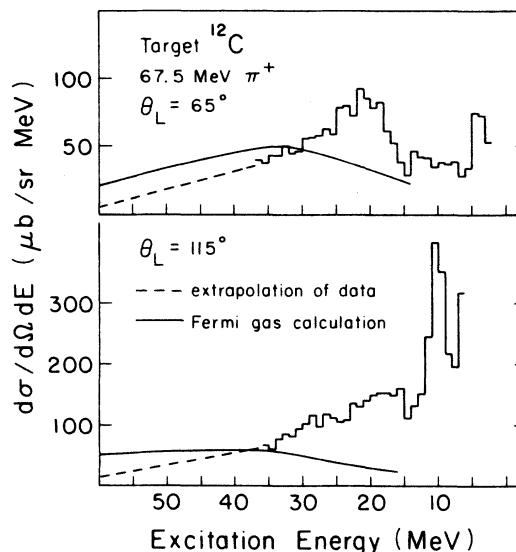

FIG. 3. Scattered π^+ spectra at $T_\pi = 67.5$ MeV emphasizing $E_x > 5$ MeV. The dashed line is the extrapolation of the data used to generate summed cross sections over all excitation energies. The solid line is a Fermi gas calculation with $N_{eff} = 5.3$ (see text).

energy window of the same width for each state. The data allowed for a straightforward determination of the 2^+ cross sections. However, the 3^- data (^{12}C) might include events from a state at 10.2 MeV that could not be resolved. The 0^+ state at 7.65 MeV could only be resolved at angles 65°−80° where it is comparable in size to the 3^-. Figure 2 shows the spectrum at 80°.

The monitoring techniques were similar to that of the previous experiment. Two large ion chambers (each 76 cm wide and 23 cm high) downstream of the target counted all particles (π, μ, e) in the beam for angle-to-angle normalization. In addition, a three-scintillator telescope was mounted at a fixed angle (60°) relative to the tar-

FIG. 2. A scattered π^+ spectrum at $T_\pi = 67.5$ MeV and $\theta_{lab} = 80°$ for ^{12}C. The solid curve under the inelastic states is the estimated background from the elastic peak.
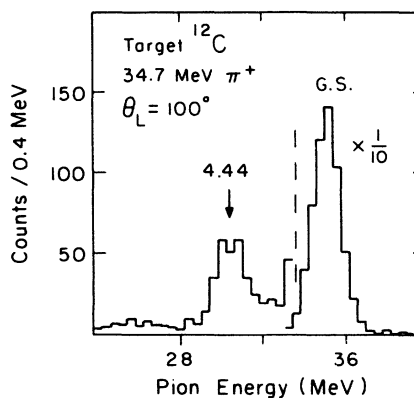

FIG. 4. A scattered π^+ spectrum for $T_\pi = 34.7$ MeV and $\theta_{lab} = 100°$ for ^{12}C.

get in the vertical plane. Its purpose was to count, on the basis of particle identification, protons from the $(\pi, 2p)$ reaction stopping in the second monitor scintillator (70–110 MeV). Although not as accurate a monitor as the ion chambers because of a nontarget-related background that had to be subtracted empirically, this device had the advantage that it was probably sensitive only to events generated by the pions in the beam. The two devices agreed to within ±10% for all points.

Absolute normalization for these data was again fixed relative to the πp scattering cross section using a CH_2 target. (See Refs. 5 and 17 for more detail.) The data of Bertin *et al.*[19] and two recent phase shift calculations[20,21] were used. The lower energy (35–50 MeV) π-nuclear data could be normalized at angles where data and calculations exist and agree well. On the other hand, the 67.5 MeV data had to be normalized at 40° where there is no data point and the two phase shift calculations disagree (see Fig. 5). An average of the two was used and a larger error (20%) than that of the data at the lower energies (15%) was assigned.

Because of the rapid change in energy of a pion scattering from hydrogen, it was possible to measure the detection efficiency for a wide range of pion energies. This is required in order to have the energy spectra properly normalized for

all excitation energies. The results are consistent with a Monte Carlo calculation that simulates the full experimental geometry and all software cuts. Although the efficiency is fairly flat within a crystal, large shifts occur at crystal interfaces. All spectra at 67.5 MeV were corrected using the calculated efficiency function. The change in efficiency relative to the elastic peak was about 15% for the 0^+ state and 20% for the 3^- state. Based on both calculation and data, no correction was deemed necessary for the 35 MeV data. (The data used were πp scattering at 50 MeV producing pions of about 30 and 34 MeV in the detector. These two measurements give relative efficiencies that agree to within 5%.) Final data for this experiment are listed in Tables I–III. The data at 48.5 MeV are listed in Ref. 5.

To generate the total inelastic cross section, the energy spectra had to be extrapolated to excitation energies not measured by the detector ($E_x < 34$ MeV). This was done in a simple empirical way in the absence of a quantitative model. All spectra slope downward for excitation energies larger than about 23 MeV. The spectra were extrapolated linearly to zero at 2 MeV kinetic energy, the Coulomb barrier. The resulting data are listed in Table IV.

III. RESULTS AND DISCUSSION

A. Elastic scattering

The elastic data for ^{12}C from this experiment are listed in Tables I and II, and shown with the
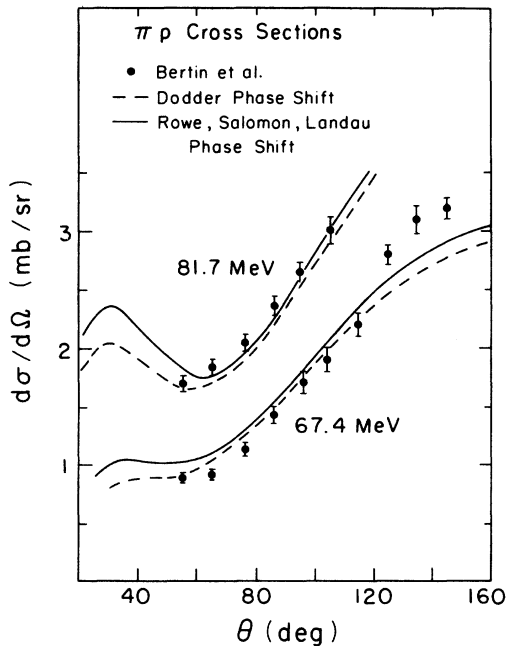

FIG. 5. A comparison of data (Ref. 19) and recent phase-shift calculations (Ref. 20 and 21) for $\pi^+ p$ scattering at 81.7 and 67.4 MeV in the laboratory system.

TABLE I. Differential cross sections for elastic (0^+) and inelastic (2^+, 4.44 MeV) scattering from ^{12}C. All quantities are evaluated in the center-of-momentum system. Cross sections are in (mb/sr) and angles in degrees. Incident π^+ energy is 34.7 MeV, the average value at the center of the target. The estimated absolute error is ±15% and is not included in the errors below.

θ	0^+ (g.s.)	2^+ (4.44 MeV)
30.4	7.10 ± 0.57	
35.5	4.51 ± 0.32	
40.6	4.02 ± 0.20	0.127 ± 0.020
45.6	3.31 ± 0.19	
50.7	3.08 ± 0.16	0.105 ± 0.015
55.8	3.02 ± 0.15	
60.8	2.89 ± 0.15	0.094 ± 0.012
65.8	3.01 ± 0.15	
70.8	3.23 ± 0.16	0.104 ± 0.013
80.9	4.26 ± 0.22	0.135 ± 0.015
90.9	5.66 ± 0.28	0.181 ± 0.022
100.9	6.74 ± 0.30	0.26 ± 0.025
110.8	7.78 ± 0.31	0.44 ± 0.05
120.8	8.74 ± 0.35	0.50 ± 0.05
145.5	9.20 ± 0.46	0.98 ± 0.09

TABLE II. Same as Table I but incident energy is 67.5 MeV. The estimated absolute error is ±20% and is not included in the errors below.

θ	0_1^+ (g.s.)	2_1^+ (4.44 MeV)	0_2^+ (7.65 MeV)	3_1^- (9.64 MeV)
25.4	29.5 ±2.5			
30.5	26.0 ±2.3	0.21 ±0.13		
35.6	20.1 ±1.5			
40.7	15.6 ±1.5	0.18 ±0.06	<0.04	
45.7	10.6 ±0.7			
50.8	6.55 ±0.4	0.15 ±0.05	<0.02	
55.9	4.66 ±0.28	0.15 ±0.05	0.024 ±0.02	
60.9	3.17 ±0.19	0.084 ±0.013	0.037 ±0.02	
66.0	2.55 ±0.12	0.087 ±0.023	0.053 ±0.015	0.04 ±0.02
71.0	2.72 ±0.14	0.095 ±0.019	0.066 ±0.033	0.025 ±0.015
76.0	3.28 ±0.16	0.185 ±0.025	0.065 ±0.032	0.082 ±0.041
81.0	3.99 ±0.20	0.222 ±0.051	0.095 ±0.031	0.10 ±0.03
91.0	5.46 ±0.37	0.481 ±0.089	0.105 ±0.05	0.19 ±0.08
101.0	4.91 ±0.40	1.12 ±0.12	0.20 ±0.06	0.61 ±0.13
116.0	4.05 ±0.32	2.16 ±0.23	0.33 ±0.16	1.30 ±0.13
130.8	2.50 ±0.25	3.59 ±0.31	0.18 ±0.13	1.97 ±0.25
140.7	1.75 ±0.18	4.05 ±0.35	0.41 ±0.20	2.4 ±0.3
150.5	1.25 ±0.13	3.97 ±0.31	0.44 ±0.22	2.2 ±0.3

data from our previous experiment[5] in Figs. 6–8. At the lowest energy, the Coulomb nuclear interference region merges with the "s-p" interference minimum[8] which is fixed at about 65°. As the energy increases, the cross sections at backward angles decrease as would be expected with the onset of diffraction effects. Table III and Fig. 9 give the data from the present silicon elastic measurement at 35.9 MeV. We have analyzed all these data using a phenomenological potential of the Kisslinger type (called KFIT in our figures), which has the following coordinate space form:

$$2EV(r)\psi(r) = -Ab_0 k^2\rho(r)\psi(r)$$

$$+Ab_1\nabla \cdot \rho(r)\nabla\psi(r).$$

The features and shortcomings of this model have

TABLE III. Same as Table I but for Si. The incident energy is 35.9 MeV. The estimated absolute error is ±15% and is not included in the errors given below.

θ	0^+ (g.s.)	2^+ (1.78 MeV)
30.2	43.8 ± 3.5	
35.2	28.5 ± 2.1	
40.2	23.0 ± 1.7	
45.3	19.4 ± 1.5	
50.3	18.4 ± 1.4	
60.3	15.5 ± 1.2	
70.4	15.4 ± 1.2	
80.4	14.9 ± 1.2	
90.4	17.1 ± 1.4	
100.4	16.6 ± 1.7	
120.3	12.9 ± 1.8	1.4 ± 0.4
140.2	10.2 ± 1.2	2.4 ± 0.7

been discussed in many places (see Refs. 1–14 and references cited therein). In our previous work, we used nuclear densities $\rho(r)$ consistent with electron scattering and varied b_0 and b_1 in a least squares fitting program[22] for a best fit to the data. Features not already present in this model are then included in a purely phenomenological way. The fits produced a single set of parameters giving a consistent description of the ~50 MeV data for ^{12}C, ^{16}O, Si, and Fe (excluding isospin effects). The biggest change from the free values was a more negative Reb_0, corresponding to greater repulsion in the effective pion-nucleon S wave.

Here we extend the fitting analysis to data at other energies ranging from 28.4 to 87.5 MeV. These data are taken from the present experiment and from Refs. 5–7 and 24. All the measurements are for π^+ except for the data of Edelstein et al.[24] at 69.5 and 87.5 MeV, which are for π^-. In fitting the UBC-TRIUMF results[6] we included only the data for angles larger than 20°, since persistent difficulties were encountered for the lesser angles. Results of this analysis are given in Table V and shown graphically in Fig. 10. Some of the fits violate unitarity, but by an amount that is not statistically significant. We note that there is little energy dependence in the ^{12}C fit parameters. The silicon data were also fit in the same way and the analysis yields values close to those obtained for ^{12}C at the same energy (see Table V).

The purposes of this analysis are limited since the derived parameters mostly have meaning in

TABLE IV. Summed inelastic ^{12}C cross sections for 67.5 MeV π^+. Each column represents a sum over a different region of excitation energies. The first two columns are based on data and the last two involve an extrapolation of the data (see text). Note that values are given in the laboratory system. An absolute error of ±20% is not included in the errors.

θ_L	σ(3–34 MeV) (mb/sr)	σ(15–34 MeV) (mb/sr)	σ(3–66 MeV) (mb/sr)	σ(15–66 MeV) (mb/sr)
25	1.2 ± 0.1	1.1 ± 0.15	1.5 ± 0.2	1.4 ± 0.3
30	1.2 ± 0.1	1.0 ± 0.12	1.4 ± 0.2	1.2 ± 0.2
35	1.2 ± 0.1	0.89 ± 0.09	1.5 ± 0.2	1.2 ± 0.2
40	1.3 ± 0.1	0.92 ± 0.03	1.7 ± 0.2	1.3 ± 0.2
45	1.2 ± 0.1	0.87 ± 0.10	1.5 ± 0.2	1.2 ± 0.15
50	1.2 ± 0.1	0.91 ± 0.10	1.6 ± 0.2	1.3 ± 0.16
55	1.4 ± 0.1	1.1 ± 0.1	1.9 ± 0.25	1.6 ± 0.2
60	1.3 ± 0.1	1.1 ± 0.1	1.8 ± 0.25	1.6 ± 0.2
65	1.5 ± 0.15	1.2 ± 0.1	2.1 ± 0.25	1.8 ± 0.2
70	1.5 ± 0.15	1.2 ± 0.1	2.1 ± 0.25	1.8 ± 0.2
75	1.7 ± 0.15	1.3 ± 0.1	2.3 ± 0.3	1.9 ± 0.2
80	2.0 ± 0.2	1.4 ± 0.1	2.7 ± 0.5	2.1 ± 0.25
90	3.0 ± 0.3	1.8 ± 0.15	3.9 ± 0.5	2.7 ± 0.3
100	4.2 ± 0.4	1.9 ± 0.15	5.1 ± 0.7	2.8 ± 0.3
115	6.8 ± 0.6	2.6 ± 0.2	8.0 ± 1.1	3.8 ± 0.4
130	9.9 ± 1.0	3.1 ± 0.25	11.4 ± 1.7	4.6 ± 0.5
140	12.1 ± 1.1	3.6 ± 0.3	13.8 ± 2.1	5.3 ± 0.6
150	11.9 ± 1.1	3.9 ± 0.3	13.8 ± 2.1	5.8 ± 0.6

relating different sets of data and providing a useful four-variable parametrization of it. Such a parametrization can provide distorted waves that are required for DWIA calculations for comparison with our inelastic data. The energy dependence of the parameters is needed since the out-
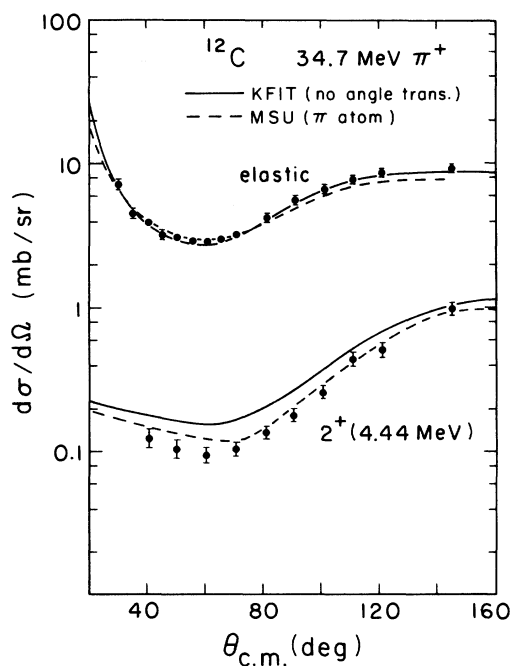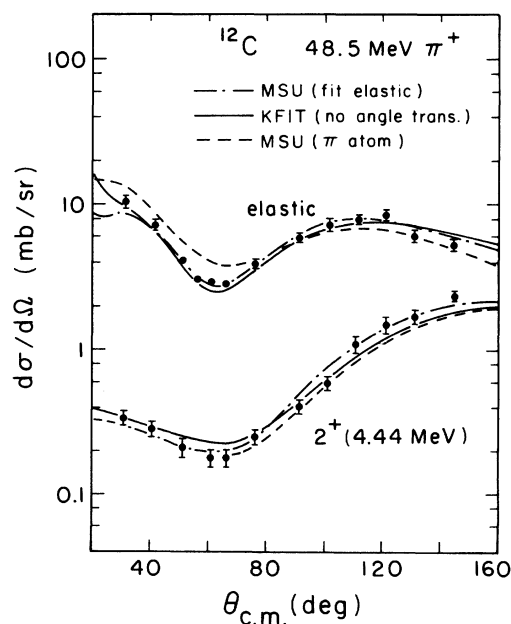

FIG. 6. The measured angular distributions for 34.7 MeV π^+ scattering to the ground state and first-excited states of ^{12}C. The solid lines use a four-parameter Kisslinger potential (labeled KFIT). The dashed curves are predictions of the MSU "pionic atom" potential A (see Ref. 12) and a standard deformed nucleus form factor with oscillator parameter $b = 1.57$ fm.

FIG. 7. Same as Fig. 6 but for 48.5 MeV π^+. In addition, curves obtained for the MSU potential by parameter adjustment are shown.
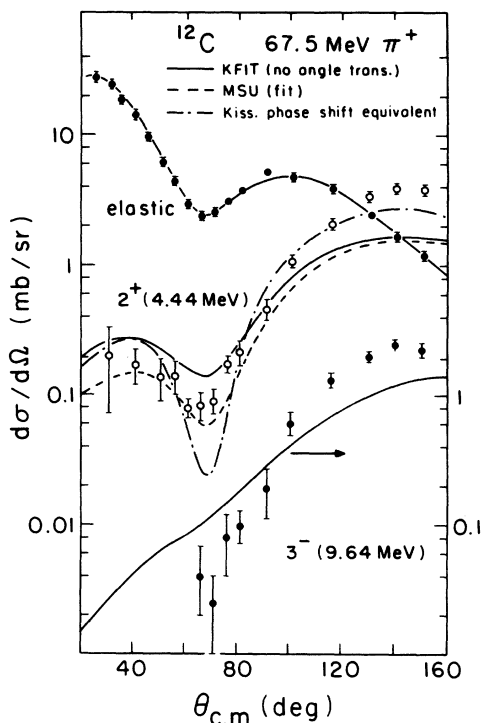
FIG. 8. The measured angular distributions for 67.5 MeV π^+ scattering from the ground state and first 2^+ and 3^- excited states of ^{12}C. The solid and dashed curves are defined in the figure legend. The dash-dot curve is the result of a phase-shift equivalent calculation; see Ref. 15 and the text. This curve has been multiplied by 2.2 to have the same magnitude as the data.

FIG. 9. The measured angular distribution for 35.9 MeV π^+ scattering to the ground and first excited 2^+ state of ^{28}Si. The solid and dashed lines are defined as in the Fig. 6 caption.

going pion for these inelastic scattering data have an energy up to 10 MeV lower than for elastic scattering.

This analysis also permits a rough gauge of the consistency of the data at different energies. This is important when the disagreement (see Refs. 5–7) for 50 MeV $\pi^+ - ^{12}$C makes it clear that the experiments are difficult. Using a linear fit (see Table VI) to the fitted parameters in Fig. 10 to recalculate cross sections gives ~10% discrepancies on the average when compared to the actual data.

Finally, a check of the consistency between π^+ and π^- can be made. The fit parameters for the present 67.5 MeV π^+ data were used to calculate 69.5 MeV π^- ^{12}C elastic scattering and the agreement with the Edelstein *et al.* data[24] is quite good, yielding a χ^2 per degree of freedom of $\frac{35}{18}$.

The large deviations between the fitted parameters and those obtained from free πN information, especially for b_0, is a measure of the deficiency of the unmodified Kisslinger potential. It is known,[25] for example, that the fitted pa-
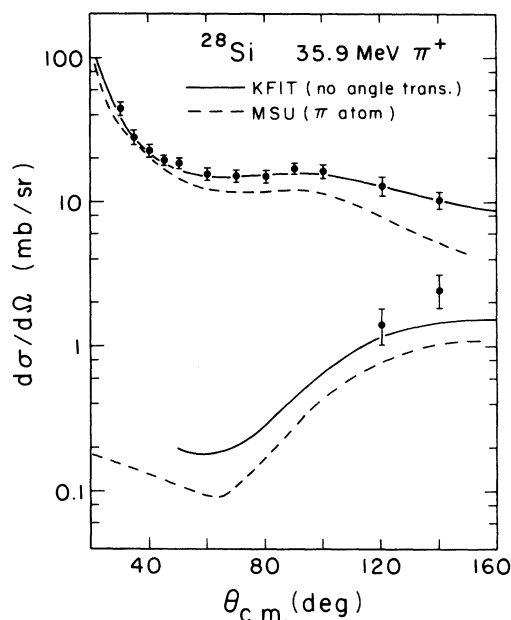
rameters provide "smoother" wave functions, devoid of some of the high momentum components due to the Kisslinger singularity. However, part of the disagreement between free and fitted parameters is due to a purely kinematic effect, the "angle transformation."[1] One of the many prescriptions for including it is to add[26] a Laplacian term to the Kisslinger potential:

$$2EV(r)\psi(r) = -Ab_0 k^2 \rho(r)\psi(r) + Ab_1 \nabla \cdot \rho \nabla \psi$$

$$- \frac{\epsilon}{2} b_1 [\nabla^2 \rho(r)] \psi(r).$$

We have also fit the data with this potential and the values for $\mathrm{Re}b_0$ are about 50% closer to the free value. Absorption terms have often been included phenomenologically with terms involving the square of the matter density. However, a recent calculation[27] of the form of the true absorption part of the optical potential gives pieces that are closer to ρ than ρ^2. Thus, a fit Kisslinger potential with an angle transformation could represent much of the relevant physics. However, due to the theoretical uncertainties and varying prescriptions used in treating this effect, we shall not present the results of a fitting analysis here.

Calculations for our data were also made by the MSU group with a fairly complicated form of optical potential[12] that has more theoretical validity. It includes s and p wave true absorption, an angle

TABLE V. Parameters for Kisslinger model calculations obtained for the data presented in this paper and Refs. 5–7 and 24. The geometrical parameters were fixed at electron scattering values (Ref. 38). Carbon was represented as a modified harmonic oscillator with b =1.67 fm and α =1.15 fm. Silicon is best described by a two-parameter Fermi shape with c =3.14 fm and a =0.54 fm. The parameters b_0 and b_1 were fit to the data in a least squares with the final chi-square given in the table. Targets were of natural isotopic abundance.

| Nucleus	Energy (MeV)	Re b_0 (fm³)	Im b_0 (fm³)	Re b_1 (fm³)	Im b_1 (fm³)	χ^2/N
			This work			
carbon	34.7	−4.0 ± 0.1	−0.12 ± 0.21	6.8 ± 0.1	1.0 ± 0.2	5/11
silicon	35.9	−4.3 ± 0.1	−0.26 ± 0.21	6.4 ± 0.4	1.2 ± 0.2	3/8
carbon	67.5	−2.7 ± 0.1	−0.40 ± 0.09	6.6 ± 0.1	1.1 ± 0.1	7/14
			Reference 5			
carbon	48.5	−3.4 ± 0.1	−0.56 ± 0.44	7.0 ± 0.1	1.6 ± 0.8	10/9
			Reference 6			
carbon	48.9	−3.4 ± 0.2	−0.45 ± 0.30	6.7 ± 0.1	1.3 ± 0.4	34/12
carbon	38.6	−3.7 ± 0.1	−0.13 ± 0.22	6.6 ± 0.2	0.95 ± 0.20	38/19
carbon	28.4	−3.5 ± 0.4	2.9 ± 0.5	6.5 ± 0.3	−0.86 ± 0.37	38/21
			Reference 7			
carbon	49.9	−3.1 ± 0.1	0.12 ± 0.14	6.5 ± 0.1	0.58 ± 0.21	18/14
carbon	40.0	−3.3 ± 0.1	0.48 ± 0.28	6.3 ± 0.1	0.46 ± 0.35	19/13
carbon	30.0	−3.9 ± 0.4	−0.90 ± 0.87	6.1 ± 0.4	1.5 ± 0.7	36/14
			Reference 24			
carbon	69.5	−2.8 ± 0.1	−0.67 ± 0.09	6.5 ± 0.2	0.80 ± 0.13	13/18
carbon	87.5	−2.1 ± 0.1	−0.80 ± 0.15	6.8 ± 0.3	1.8 ± 0.1	15/17
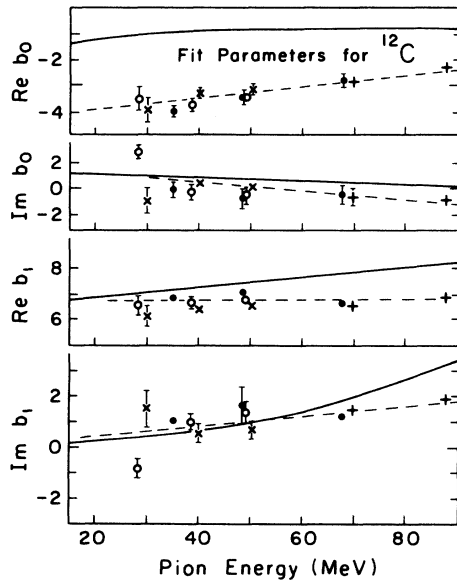
FIG. 10. Real and imaginary parts of b_0 and b_1 as a function of energy for the zero-range Kisslinger potential as determined from experiments on ^{12}C. The data from this experiment (solid dots), from Ref. 6 (open dots), from Ref. 7 (crosses), and from Ref. 24 (plusses) have all been analyzed using the same potential form to obtain this graph. The solid lines are obtained from the free pion-nucleon phase shifts. The dashed lines are straight line best fits; see Table VI.

transformation, Pauli blocking, and the Lorentz-Lorenz-Ericson-Ericson effect. Results from such calculations are shown in Figs. 6–9. Nevertheless, a certain amount of phenomenology is still required to fit the data.

B. Inelastic scattering to low-lying collective states

Differential cross sections for the formation of 2^+ and 3^- states in ^{12}C at 4.44 and 9.64 MeV are shown in Figs. 6–8. These highly collective states have been studied with other projectiles for many years and their wave functions are well understood, making them attractive candidates for studies of pion dynamics. The 2^+ cross section is large enough to measure at all our energies and angles, but the 3^- is very small at forward angles and low energies. Each 2^+ distribution

TABLE VI. The results of straight-line best fits to the values of b_0 and b_1 presented in Fig. 10. The data for each parameter has been fit to a line of the form $a + bE$, with the laboratory kinetic energy in MeV.

Parameter	a (fm³)	b (fm³/MeV)
Re(b_0)	−4.8 ± 1.1	0.031 ± 0.002
Im(b_0)	1.0 ± 0.21	−0.022 ± 0.003
Re(b_1)	6.6 ± 1.6	0.0008 ± 0.003
Im(b_1)	−0.22 ± 0.2	0.021 ± 0.003

has a minimum at ~65° that gets sharper as the
energy increases, much like the elastic distribu-
tion. At all three energies, the cross sections
for angles greater than 80° rise steeply while the
elastic cross section tends to be decreasing. This
is expected since the form factor for this state,
measured with electron scattering,[28] has a peak
at 1.1–1.3 fm^{-1}, the range in momentum transfer
that contributes to the largest angles at 67.5
MeV. Cross sections for the 3$^-$ state also rise
at back angles for the same reason. A few data
points for the 2$^+$ state at 1.78 MeV in ^{28}Si were
also measured at 35.9 and 49.3 MeV. This state
is also highly collective and well studied with
other projectiles. Therefore, these data also
could provide a test of pion optical models.

Calculations describing these data have been
made within the distorted wave impulse approxi-
mation (DWIA).[23,29] An isoscalar state of multi-
polarity λ and normal parity is excited in a single
step by a transition operator,

$$V_{tr}(q) = t_{\pi N} F_\lambda(q) ,$$

where $t_{\pi N}$ is the same pion-nucleon scattering
operator used in the optical potential. F_λ is the
form factor describing the probability for the
nucleus to change states by absorbing momentum
q from the incident particle. The inelastic cross
section is then given by

$$\frac{d\sigma}{d\Omega} \sim |\langle\chi_f^{(-)}|\langle\lambda| V_{tr}|0\rangle|\chi_i^{(+)}\rangle|^2 ,$$

with the χ being the distorted pion wave functions,
and $\langle\lambda| V_{tr}|0\rangle$ being the nuclear transition density.
Note that the pion dynamics occur in both the
distorted waves and in the transition operator.
Two models can then produce the same distorted
wave functions yet different cross sections. It
should also be noted that pions have a quite dif-
ferent transition operator V_{tr} than other pro-
jectiles because of the derivatives in $t_{\pi N}$.

A collective form factor can be derived by as-
suming the excited state mass distribution is the
same as that of the ground state but with a
macroscopic deformation of the proper multi-
polarity

$$F_\lambda(r) = \beta_\lambda b \frac{\partial \rho}{\partial b} ,$$

where β_λ is a strength parameter and ρ is the
ground state density with harmonic oscillator
parameter b. This simple model agrees well
with a phenomenological form factor that fits
older electron and proton scattering data for these
states at the momentum transfers relevant to this
experiment.[30] Values for β_λ were taken from
previous hadron scattering results (^{12}C:

$\beta_2 = 0.56$; $\beta_3 = 0.40$; ^{28}Si: $\beta_2 = 0.40$).[31]

As was stressed in our previous paper, the use
of an optical potential (πN t matrix) that fits the
elastic data is essential for calculating inelastic
cross sections. We use the potentials described
in the previous section which were fitted to the
elastic data. The energy of the outgoing pion is
up to 10 MeV lower than that of the incoming pion
and the optical potential parameters used in each
case were chosen with reference to Fig. 10. Our
parameters for the new data at 35 and 67 MeV
are given in Table V.

Results obtained with the fit Kisslinger potential
are shown as the solid line in Figs. 6–8 for ^{12}C
and Fig. 9 for ^{28}Si. The ^{12}C data for the 2$^+$ is
described better at the two lower energies than
at 67.5 MeV, where the 2$^+$ prediction falls more
than a factor of 2 below the data at the back ang-
les. A similar problem is encountered with the 2$^+$
data of Edelstein et al.[24] at 69.5 MeV. The 3$^-$
calculation at the same energy has the same dif-
ficulty at back angles and is also somewhat larger
than the data at forward angles. As at 49.3 MeV,
the silicon 2$^+$ data are sparse and test no more
than the absolute magnitude of the calculation.
At each energy, the calculation is somewhat low.
The curves labeled MSU (π atom) were calculated
with a potential[12] that was fit to pionic atom data
and includes energy dependence. The predictions
are quite good for the 34.7 MeV carbon data, but
progressively worse at 48.5 and 67.5 MeV. Thus,
it would seem to be a good potential for pion ener-
gies of less than about 60 MeV for ^{12}C. However,
the MSU (π atom) model also misses the elastic
data for silicon, a 0$^+$ $T = 0$ nucleus like ^{12}C, at
35.9 MeV.

Some tests of dependence of the ^{12}C 2$^+$ cross
section on the optical potential were carried out,
especially with regard to explaining the discrep-
ancy of the DWIA at 67.5 MeV. Using the Kiss-
linger potential including the angle transformation
to fit the elastic data produces no significant
change at any energy of this experiment. Despite
the greatly different form of the MSU potential,
its inelastic predictions are quite close to those
of the Kisslinger model if both are constrained
to fit the elastic data.

As discussed in the Introduction, a fit to elastic
data does not uniquely determine the pion wave
function within the nucleus. Keister[15] has tested
this property by transforming the interior wave
function while maintaining phase shift equivalence
and finds that the shape of the inelastic angular
distribution can be significantly altered. An ex-
ample is shown in Fig. 8 where only the π-nucleus
p wave phase was changed (at the center of the
nucleus by 25° and progressively less for larger

radii). The transformed distribution has a shape
similar to the data, but had to be multiplied by
2.2 to reproduce the absolute magnitude.

Another possible explanation for the discrepancy
at 67.5 MeV is a breakdown of the DWIA. Both
the 2^+ and 3^- are larger than the elastic at the
back angles indicating that the coupling is quite
strong to these states. A coupled channels calcu-
lation might give a better description.

The data for the 0^+ state at 7.65 MeV is shown
in Fig. 11. It is not well resolved at most angles
and the estimated errors are subsequently large.
At angles less than 55°, only upper limits could
be established. Unlike the levels previously
discussed, the nuclear structure for this state
is not well understood. Sparrow and Gerace[32]
used a form factor that fit electron scattering
data to this state, and a Kisslinger potential with
an angle transformation for calculations at 50
MeV. Their DWIA result was an order of magni-
tude higher than the data,[5] but a coupled channels
calculation produced a strong interference of the
one-step $(0_1^+ \rightarrow 0_2^+)$ with the two-step $(0_1^+ \rightarrow 2_1^+ \rightarrow 0_2^+)$
excitation and the absolute magnitude then agreed
with the data. Although the data were taken at
only 5 angles and the error bars were large, the
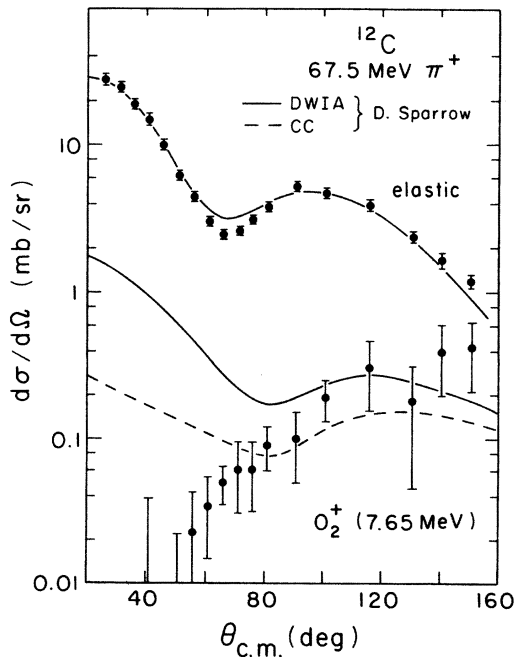calculation seemed to have more structure than

FIG. 11. The measured angular distributions for 67.5
MeV π^+ scattering to the ground state and 0^+ (7.65 MeV)
state. The calculations are by Sparrow (see Ref. 32),
the optical potential used was developed by the Colorado
group (Ref. 13), and the form factor for the DWIA and
coupled channels (cc) calculations was taken from fits
to electron scattering (Ref. 28).

the data.

A similar calculation was made[32] (but with a
Colorado optical potential) for our new data and
the results are similar. The DWIA calculation
does well at angles larger than 100° but badly
misses the forward angle data. The coupled
channels calculation is now reduced by about a
factor of 3 from the DWIA, but definitely has
the wrong shape. The data are again much lower
at forward angles. Hopefully, the two data sets
that now exist for this state can further constrain
the complicated pion dynamics involved in this
calculation.

C. Inclusive inelastic cross sections

Two sample inelastic spectra (65° and 115°)
at $T_\pi = 67.5$ MeV are shown in Fig. 3, emphasiz-
ing the data at high excitation energies. In the 65°
spectrum, there is a prominent bump at $E_x \sim 21$
MeV, which is the region where we expect
$[1p_{3/2}^{-1}, (2s1d)]$ states. Since it is significantly
wider than the energy resolution (~3 MeV), it is
probably at least two unresolved states. Strongly
excited 2^- and 4^- $(T = 0, 1)$ states have been seen
with pions and electrons[33,34] at $E_x \sim 19$–20 MeV.
In addition, the giant dipole resonance has been
seen in ^{12}C at $E_x \sim 23$ MeV.[35] Cross sections for
the bump seen in this data are difficult to deter-
mine because of its width and background. With a
smooth background, values of a few tenths of a
millibarn per steradian are obtained at angles
from 30° to 80°.

Since the data was taken with moderate resolu-
tion, its main value at the higher excitation ener-
gies is in the three body continuum above the
nucleon emission threshold at $E_x = 16$ MeV. This
continuum is probably dominated by processes
involving a single pion-nucleus collision since the
pion interacts so weakly at this energy. However,
this interaction will be somewhat different than
the free πN case because nuclear structure effects
should be significant at these low momentum
transfers $(q \lesssim 1.6 \text{ fm}^{-1})$. To examine how closely
the quasifree picture applies to this data, we have
used a Fermi gas model. The nucleus is treated
as a group of independent particles. A scattering
event has the same cross section as for free
pions and nucleons,[35] but the struck nucleon must
end up with momentum above the Fermi momen-
tum (221 MeV/c in carbon). The cross section
can be represented as

$$\frac{d^2\sigma}{d\Omega dE} = N_{eff} R_F(q, \omega) \frac{d\sigma}{d\Omega}\bigg|_{\pi N}.$$

$d\sigma/d\Omega|_{\pi N}$ is the pion-nucleon cross section at the
same incident energy and angle. R_F is the Fermi
gas form factor for a single nucleon. N_{eff} is the

multiplicative factor that has been interpreted as the effective number of nucleons participating in the reaction. This model works very well for electron scattering at momentum transfers well above the Fermi sea,[35] but not at momentum transfers comparable to those of this experiment[36] ($q \lesssim 300$ MeV/c).

An example of a calculated energy distribution (N_{eff} = 5.3) is given in Fig. 3; it does not look much like the data. This is an indication that nuclear structure effects are very important at least below 30 MeV excitation.

The Fermi gas angular distribution is shown in Fig. 12 along with the data for the energy integrated, $3 < E_x \lesssim 66$ MeV and $15 < E_x \lesssim 66$ MeV, angular distributions. The latter energy cut gives a close approximation to the total continuum strength and is the appropriate data for comparison with the Fermi gas calculation. Normalizing the calculation to the 15–66 MeV data at 80° gives N_{eff} = 5.3. The agreement is then fairly good, although the strong disagreement observed in the energy distributions is masked.

The average $\pi^+ N$ cross section is also shown in Fig. 12, normalized at 80° as the Fermi gas calculation. The difference between the two calculations involves the inclusion of effects due to binding energy and the Pauli principle. This seems to have only a small effect on the shape of the angular distribution except at angles less than 50°.

Finally, the data can be summed over angles to produce a total inelastic cross section. This was

done by fitting the angular distribution to a Legendre polynomial series. As higher order terms are added to the fit, the chi-square reached a minimum and a fairly constant total cross section with about 4 terms. Including a number larger than about 7 produced spurious structure in the fitted distribution. The measured total inelastic cross section for 67.5 MeV π^+ and ^{12}C is 73 ± 25 mb.

Some calculations have been made for this quantity. The MSU (Ref. 12) group distinguish between the absorptive and the inelastic scattering terms in their potential and used the formula

$$\sigma^{tot}(qe) = -\frac{2}{v_\pi} \langle \psi | \mathrm{Im} V(qe) | \psi \rangle .$$

The terms of the optical potential used represent only nucleon knockout processes and therefore should underestimate the total inelastic cross section. The MSU group obtains a value of 89 mb for the total inelastic cross section. Thomas and Landau[37] made a calculation under the assumption of a first order potential and no absorption that they describe as indicative of the total inelastic cross section. They note strong sensitivity to nuclear medium corrections in their results. The result for their best model is 56 mb. Both are within the large error bars we quote. It is clear that much additional work is needed on both the experimental and theoretical sides if this is to be a good test of scattering models. A reasonable calculation should include scattering and absorption effects in a consistent way; these kinds of data should provide a good test of this consistency.

IV. SUMMARY

Data have been presented that greatly add to the body of low energy pion inelastic scattering information. New measurements include $\pi^+ + ^{12}$C at 34.7 and 67.5 MeV and $\pi^+ + ^{28}$Si at 35.9 MeV.

All low energy elastic scattering data[6,7,24] for ^{12}C were analyzed within the Kisslinger model as for our previous measurement.[5] The four parameters (b_0, b_1) were varied freely to give the minimum chi-square for each data set. The parameters derived were quite different from the free values (as before) but the trend with energy is quite similar to that of the free values.[20] We find that both π^+ and π^- ^{12}C data at ~68 MeV yield the same (b_0, b_1) values, as would be expected for a $T = 0$ target if we neglect the Coulomb interaction. We also find that the addition of an angle transformation can account for much of the large discrepancy in Re b_0 between free and phenomenological values.
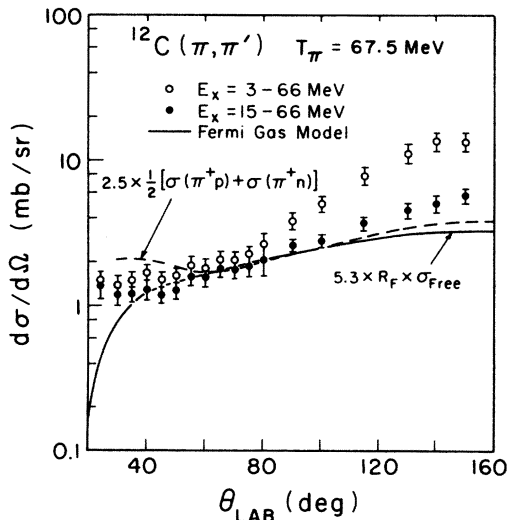

FIG. 12. The inelastic cross section summed over the energy regions given in the legend. The solid curve is the prediction of a Fermi gas calculation, with N_{eff} = 5.3, while the dashed curve is 2.5 times the average free πN cross section.

A DWIA analysis was presented for the collective states using form factors that fit electron scattering data. Three different types of optical potential were used to generate the distorted waves. The fit Kisslinger potentials (with and without the angle transformation) give very similar inelastic predictions. The model developed by the MSU group[12] has much greater theoretical viability and its predictions fit the data better than the Kisslinger calculations if the potential is adjusted to fit the elastic channel information. However, each calculation falls over a factor of 2 below the data for the 2^+ (4.4 MeV) state at back angles at 67.5 MeV. At this time, possible inadequacies in the pion potential and the DWIA formalism cannot be separated.

Both DWIA and coupled channel calculations by Sparrow[32] were compared to data for the 0_2^+ state in ^{12}C. Neither calculation does well and inadequacies in the details of the coupled channels calculation are more clear for the new data. This case appears to provide a stringent test of pion scattering dynamics and/or our understanding of the nuclear structure of this state.

The summed inelastic cross sections present a good test of pion theories. The data were taken at 67.5 MeV incident π^+ energy, and the resulting spectra extend up to 34 MeV excitation energy in the residual nucleus. Integrated cross sections are obtained after summing first over excitation energy and then scattering angle. Summing should average over complicated details of the interaction and test the theory for more general features.

Quasifree pion nucleon scattering calculations give the general shape of the inelastic angular distribution for events with $E_x \geq 15$ MeV, but fall ~50% below the data at back angles and show little improvement over the shape of the free πN cross section. Furthermore, quasifree calculations of the energy spectrum at a specific angle bear little resemblance to the data. This suggests that quasifree scattering is significantly altered by nuclear structure and/or pion distortion effects.

The total inelastic cross section was estimated for 67.5 MeV π^+ ^{12}C to be 73 ± 25 mb. Within its large error bars, we cannot resolve the discrepancy between two recent calculations. Significant improvements in both theory and experiment are foreseen as necessary before successful tests of theory are possible.

ACKNOWLEDGMENTS

*Present address: Los Alamos Scientific Laboratory, Los Alamos, N. M. 87545.

†Present address: Physics Dept., Massachusetts Institute of Technology, Cambridge, Mass. 02139.

[1] A. W. Thomas and R. H. Landau, Phys. Rep. **58**, 121 (1980).

[2] R. H. Landau, in *Proceedings of the ith International Conference on High Energy Physics and Nuclear Structure*, edited by A. W. Thomas and D. F. Measday (North-Holland, Amsterdam, 1980).

[3] R. Redwine, in *Meson Nuclear Physics — 1979 (Houston)*, edited by E. V. Hungerford III (AIP, New York, 1979).

[4] B. Preedom, in *Proceedings of the 7th International Conference on High Energy Physics and Nuclear Structure*, edited by M. P. Locher (Birkhauser, Basel, 1979), p. 119.

[5] S. A. Dytman, J. F. Amann, P. D. Barnes, J. N. Craig, K. G. R. Doss, R. A. Eisenstein, J. D. Sherman, W. R. Wharton, R. J. Peterson, G. R. Burleson, S. L. Verbeck, and H. A. Theissen, Phys. Rev. Lett. **38**, 1059 (1977); **39**, 53(E) (1977); Phys. Rev. C **18**, 2316 (1978); **19**, 971 (1979).

[6] R. R. Johnson, T. G. Masterson, K. L. Erdman, A. W. Thomas and R. H. Landau, Nucl. Phys. **A296**, 444 (1978); R. R. Johnson, T. Masterson, B. Bassalleck, W. Gyles, T. Marks, K. L. Erdman, A. W. Thomas, D. R. Gill, E. Rost. J. Kraushaar, J. Alster, C. Sabev, J. Arvieux, and M. Krell, Phys. Rev. Lett. **43**, 844 (1979).

[7] M. A. Moinester, R. L. Burman, R. P. Redwine, M. A. Yates-Williams, D. J. Malbrough, C. W. Darden, R. D. Edge, T. Marks, S. H. Dam, B. M. Preedom, F. E. Bertrand, T. P. Cleary, E. E. Gross, C. A. Ludemann, M. Blecher, K. Gotow, D. Jenkins, and F. Milder, Phys. Rev. C **18**, 2678 (1978). D. J. Malbrough, C. W. Darden, R. D. Edge, T. Marks, B. M. Preedom, F. E. Bertrand, T. P. Cleary, E. E. Gross, C. A. Ludemann, K. Gotow, R. L. Burman, M. A. Moinester, and R. P. Redwine, Phys. Rev. C **17**, 1395 (1978). M. Blecher, K. Gotow, D. Jenkins, F. Milder, F. E. Bertrand, T. P. Cleary, E. E. Gross, C. A. Ludemann, M. A. Moinester, R. L. Burman, M. Hamm, R. P. Redwine, M. Yates-Williams, S. Dam, C. W. Darden III, R. D. Edge, D. J. Mal-

brough, T. Marks, and B. M. Preedom, Phys. Rev. C **20**, 1884 (1979).

[8]M. D. Cooper and R. A. Eisenstein, Phys. Rev. C **13**, 1334 (1976).

[9]R. H. Landau, S. C. Phatak, and F. Tabakin, Ann. Phys. (N.Y.) **78**, 299 (1973).

[10]R. H. Landau and A. W. Thomas, Nucl. Phys. **A302**, 461 (1978).

[11]L. C. Liu and C. M. Shakin, Phys. Rev. C **19**, 129 (1979); **16**, 333 (1977).

[12]K. Stricker, H. McManus, and J. Carr, Phys. Rev. C **19**, 929 (1979); K. Stricker, J. A. Carr, and H. McManus, *ibid.* **22**, 2043 (1980).

[13]N. DiGiacomo, A. S. Rosenthal, E. Rost, and D. A. Sparrow, Phys. Lett. **66B**, 421 (1977).

[14]G. E. Brown, B. K. Jennings and V. I. Rostokin, Phys. Rep. **50**, 227 (1978).

[15]B. K. Keister, Phys. Rev. C **18**, 1934 (1978); unpublished; private communication.

[16]K. Aniol, D. Chiang, I. Halpern, D. Storm, R. Eisenstein, W. Wharton, N. Colella, R. Grace, S. Dytman, K. Doss, D. Marlow, F. Takeutchi, P. Barnes, C. Ellegaard, J. Amann, M. Cooper, and L. Knutson, Bull. Am. Phys. Soc. **25**, 505 (1980); and to be published.

[17]S. A. Dytman, Ph.D. thesis, Carnegie-Mellon University, 1978.

[18]K. G. R. Doss, Ph.D. thesis, Carnegie-Mellon Universith, 1980.

[19]P. Y. Bertin, B. Coupat, A. Hivernat, P. B. Isabelle, J. Duclos, A. Gerard, J. Miller, J. Morgenstern, J. Picard, P. Vernin, and R. Powers, Nucl. Phys. **B106**, 341 (1976).

[20]G. Rowe, M. Salomon, and R. H. Landau, Phys. Rev. C **18**, 584 (1978).

[21]D. Dodder, private communication.

[22]M. D. Cooper and R. A. Eisenstein, LASL Report No. LA-5929-MS (unpublished).

[23]R. A. Eisenstein and G. A. Miller, Comput. Phys. Commun. **11**, 85 (1976).

[24]R. M. Edelstein, W. F. Baker, and J. Rainwater, Phys. Rev. **122**, 252 (1961).

[25]G. A. Miller, Nucl. Phys. **A224**, 269 (1974).

[26]G. A. Miller, Phys. Rev. C **10**, 1242 (1974).

[27]L. S. Kisslinger and A. N. Saharia, Phys. Rev. C **22**, 1202 (1980).

[28]H. L. Crannell, Phys. Rev. **148**, 1107 (1966).

[29]T. S. H. Lee and F. Tabakin, Nucl. Phys. **A226**, 253 (1974).

[30]R. M. Haybron, M. B. Johnson, and R. J. Metzger, Phys. Rev. **156**, 1136 (1967).

[31]P. H. Stelson and L. Grodzins, At. Data Nucl. Data Tables **1**, 29 (1965).

[32]D. A. Sparrow and W. J. Gerace, Phys. Rev. Lett. **41**, 1101 (1978); private communication.

[33]H. A. Thiessen, Nucl. Phys. **A335**, 329 (1980) and references therein.

[34]E. R. Siciliano, Los Alamos Report No. LA-7892-C, p. 92.

[35]T. W. Donnelly and J. D. Walecka, Annu. Rev. Nucl. Sci. **25**, 329 (1975).

[36]W. Czyz, Phys. Rev. **131**, 2141 (1963).

[37]A. W. Thomas and R. H. Landau, Phys. Lett. **77B**, 155 (1978).

[38]C. W. De Jager, H. De Vries, and C. De Vries, At. Data Nucl. Data Tables **14**, 479 (1974).